electronics

MDPI

Article

Sensitivity Enhancement of a PPM Level Capacitive Moisture Sensor

Lokesh Kumar [1], Tarikul Islam [2,*] and Subhas Chandra Mukhopadhyay [3]

[1] Department of Physics & Astrophysics, University of Delhi, Delhi-110007, India; lok17@rediffmail.com
[2] Department of Electrical Engineering, Faculty of Engineering & Technology, Jamia Millia Islamia (A Central University), Maulana Mohammed Ali JauharMarg, New Delhi 110025, India
[3] Department of Mechanical/Electronics Engineering, Macquarie University, Sydney, NSW 2109, Australia; subhas.mukhopadhyay@mq.edu.au
* Correspondence: tislam@jmi.ac.in; Tel.: +91-11-2698-1717 (ext.2355)

Academic Editor: Mostafa Bassiouni
Received: 21 March 2017; Accepted: 16 May 2017; Published: 20 May 2017

Abstract: Measurement of moisture at ppm or ppb level is very difficult and the fabrication of such sensors at low cost is always challenging. High sensitivity is an important parameter for trace level (ppm) humidity sensors. Anelectronic detection circuit for interfacing the humidity sensor with high sensitivity requires a simple hardware circuit with few active devices. The recent trends for increasing the sensitivity include fabricating nanoporous film with a very large surface area. In the present work, the sensitivity of a parallel plate capacitive type sensor with metal oxide sensing film has been significantly improved with an aim to detect moisture from 3 to 100 ppm in the industrial process gases used to fabricate semiconductors and other sensitive electronic devices. The sensitivity has been increased by (i) fabricating a nanoporous film of aluminum oxide using the sol-gel method and (ii) increasing the cross-sectional area of a parallel plate capacitor. A novel double sided capacitive structure has been proposed where two capacitors have been fabricated—one on the top and one on the bottom side of a flat alumina substrate—and then the capacitors are connected in parallel. The structure has twice the sensitivity of a single sensor in the same ppm range but the size of the structure remains unchanged. The important characteristics of the sensors such as the sensitivity ($S = \frac{\Delta C}{\Delta ppm} \times 100$), the response time ($t_r$), and the recovery time (t_c) are determined and compared with a commercial SHAW, UKdew point meter. The fabricated double sided sensor has comparable sensitivity (S = 100%, t_r (s) = 28, t_c (s) = 40) with the commercial meter (S = 100.5%, t_r (s) = 258) but has a faster response time. The proposed method of sensitivity enhancement is simple, and mass producible.

Keywords: porous alumina; sol-gel technique; capacitive sensor; sensitivity; dynamic range; ppm

1. Introduction

Humidity sensors are widely used in different industrial, agricultural, medical, food preservation, home ventilation and air-conditioning (HVAC), and respiratory monitoring applications for the development of smart cities. Moisture measurement at ppm level is essential for condition monitoring of gas insulated substations (GISs), transformers, and circuit breakers in orderto achieve uninterrupted power supply in smart cities. The trace moisture sensor is extremely useful in certain crucial applications, where it can withstand corrosive and contaminating gases. The sensor should be sensitive to sudden and drastic change of moisture and available at low cost with a relatively long calibration period. The dynamic range of humidity measurement, which extends from %RH to ppb level, is extremely large [1–5]. Capacitive sensors are widely used for the measurement of humidity

over a wide range. The most widely used capacitive sensor in %RH is the interdigitated electrode structure. The interdigitated sensor, to the best of our knowledge, is only suitable for RH level humidity measurement [5]. Very recently, an attempt has been made by the authors to measure moisture at ppm level by a micro interdigitated capacitive sensor. However, the sensor does not show sensitivity less than 200 ppm [6]. A large number of research articles is published every year in different journals on the topic of %RH humidity measurement. However, the number of research papers for ppm level moisture detection is very low [5]. The cost of a commercial ppm level moisture sensor is at least fifty times higher than that of RH sensors [6,7].

Aluminum oxide may be suitable for trace level moisture measurement, since it is thermally stable, and chemically inert in a corrosive environment. Among the different methods of alumina film preparation, the sol-gel method is a simple, less expensive method to prepare a pure ceramic thin film of desired thickness. The film can be formed on the ceramic substrate by the dip coating, spin coating or spray coating method [1,2,6–10]. Incomparison to other ceramic materials, aluminum oxide (Al_2O_3) is highly hydrophilic and it is one of the most useful materials for moisture measurement in most industrial gases [4,10,11]. Several works have been reported in the recent past to measure moisture in the range of 0–100 ppm. However, enhancement of the sensitivity is still required to make a prototype system for the possibility of commercial applications. In addition, there is a need to increase the dynamic range below 10 ppm [8,9,12–23]. Continuous efforts are made by the researchers to fabricate highly porous nanostructures such as nanowire, nanotubes, and nanopores using different fabrication techniques. Such nanostructure films result in a very high surface area suitable for humidity sensing [23–29]. Efforts are also being made to explore new fabrication techniques and materials to achieve the goal of high sensitivity and selectivity [30]. The methods followed for the fabrication of nanostructures with desirable pore morphology are costly, time consuming and very often lead to failure. It is not necessary that the sensitivity will increase by increasing the surface area. It also requires tuning the pore morphology. Most recently, the sensitivity of a capacitive trace moisture sensor was enhanced by increasing the surface area of a pure alumina nanoporous film with the addition of polymer polyethylene glycol (PEG). The surface area of the alumina is increased two-fold but the sensitivity is increased by approximately 61%. It is found that with the increase in surface area, the size of the pores also increases [8].

In the present work, we have studied the sensitivity of a capacitive trace moisture sensor for measuring moisture in ppm. The sensitivity has been addressed by (i) selecting a suitable pore morphology nanostructured thin film of Al_2O_3; and (ii) increasing the cross-sectional area of the parallel plate electrode. To enhance sensitivity further, a unique structure with two identical parallel plate capacitors on each side of the alumina substrate has been fabricated. When these two capacitors are connected in parallel, the sensitivity is enhanced almost two-fold but the actual size remains unchanged. Also, this structure prevents the wastage of very useful dip-coated film on the opposite side of the substrate as reported previously in [7,9,14,16,17,21–23]. The proposed method of sensitivity enhancement is easy, simple, and less time consuming. The sensor can be utilized for condition monitoring of electrical equipment and moisture measurement in human respiration.

2. Experimental

2.1. Preparation of the Sol for the Al_2O_3 Sensing Film

Material aluminum hydroxide or Boehmite (AlO(OH)) sol was prepared by the addition of aluminum secondary butoxide ($C_{12}H_{27}AlO_3$) precursor into an excess amount of warm DI (Deionized) water [8,9,31,32]. The molar ratio of alumina precursor to water was fixed at approximately 1:100. The solution was initially hydrolyzed for nearly 1 h with continuous stirring on a magnetic hot plate stirrer at a constant temperature of 90 °C. The solution was then peptized by adding concentrated hydrochloric (HCl) acid drop wise with the molar ratio ~0.07 mol/mol. During peptization, the hydroxide molecules are positively charged ($Al(OH)_3^+$) and are dispersed uniformly in the colloidal

solution. The dispersed ions form a net structure and after complete peptization, the sol becomes transparent. To remove the excess volatile organic impurities from the sol, the solution was refluxed for about 18 h at a constant temperature of 80 °C.Finally, the solution was stirred on a magnetic hot plate for nearly 24 h at a room temperature of 25 °C. To facilitate the adhesion of the film on the substrate, nearly 1% polyvinyl alcohol (molecular weight 125,000) was mixed in the sol solution.

2.2. Microstructures of the Porous Aluminum Oxide

Pore morphology of the γ-Al_2O_3 film was characterized by powder X-ray diffraction (PXRD), field emission electron microscope (FESEM) and Brunauer–Emmett–Teller (BET) surface area and a pore size analyzer respectively. X-ray diffraction and BET analysis were carried out using a powder sample of the ceramic. Powder ceramic samples were prepared from the fixed amount of sol solution. The solution was dried initially at 80 °C and then sintered for 1 h at different temperatures of 450 to 550 °C. XRD analysis was carried out with a Bruker D8 advance diffractometer using Ni filtered Cu-Kα radiation (λ = 1.54056 Å, 2θ = 20° to 80°) with a scanning rate of 0.05°/s. An XRD diffractogram of the sample sintered at 450 °C for 1 h is shown in Figure 1. The sample shows multiple XRD peaks showing the presence of γ-Al_2O_3 phase. However, the diffraction peaks were broad, indicating the small size of the crystals. The XRD peaks are almost identical to the peaks obtained from the sample sintered at the temperature of 450 °C for 6 h [9]. During sintering, aluminum hydroxide undergoes a number of polymorphic phase transformations. Finally, it is converted to highly stable α-alumina phase at around 1000 °C [9,31]. Debye–Scherrer's equation was used to calculate the average crystallite size from the strongest XRD peak, as shown in Figure 1.

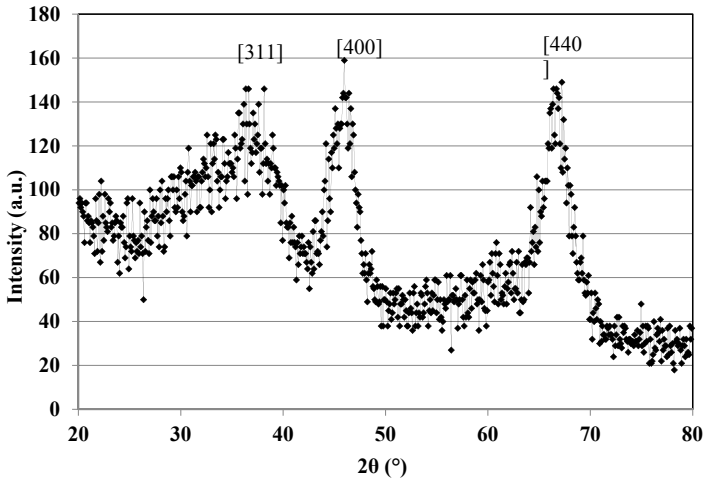

Figure 1. XRD results of the alumina powder prepared from the sol-gel method showing γ-Al_2O_3 (450 °C, 1 h).

The average size of the crystallite was found to be ~4 nm. The BET gas adsorption and desorption method was used to determine the surface area of the powder samples. The nitrogen gas adsorption isotherm of the sample is shown in Figure 2 [11,12].The isotherm was studied using a Nova 2000e (Quantachrome Instruments Limited, Boynton Beach, FL, USA) BET analyzer at liquid nitrogen temperature (77 K). The oxide sample in power form was placed in a sample cell and allowed to degas for nearly 2 h at 250 °C in vacuum. The degassed material was then exposed to a known concentration of N_2 gas at the constant temperature. The adsorption isotherm plotted between 1/[W((Po/P)-1)] and relative pressure P/P0 for γ-Al_2O_3 is shown in Figure 2.

The specific surface area, the average pore size and the micro-pore volume of the samples sintered at different conditions are shown in Table 1.

It is observed that with the increase in sintering time and temperature, the BET surface area reduces and the DA (Dubinin Astakhov) pore size increases. The roughness of the porous film

deposited on an alumina substrate (α-phase) was determined by the atomic force micrograph (AFM). The microstructure of the alumina film deposited on the substrate was also studied using FESEM. The FESEM image of the top surface of the metal oxide film at 100 nm scale is shown in Figure 3. The surface contains a large number of voids (micropores) of different sizes. The average pore size of the voids is around 10 nm.

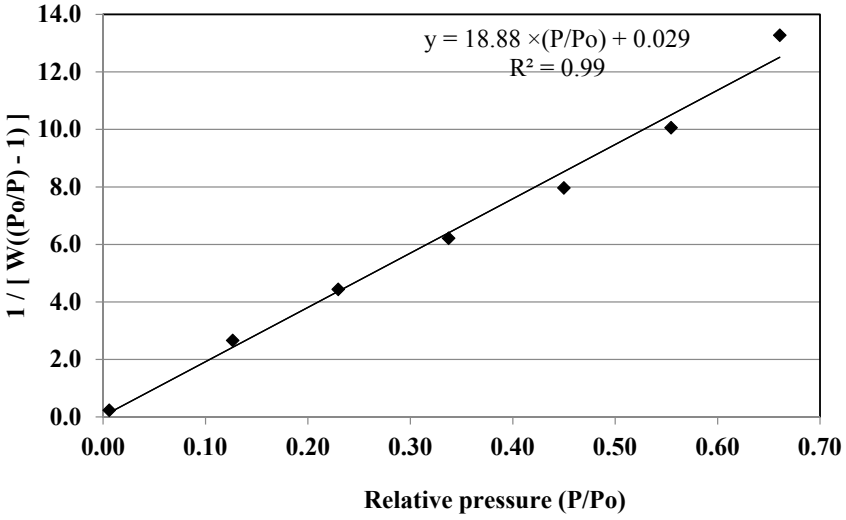

Figure 2. N_2 gas adsorption plot of the γ-Al_2O_3 film (450 °C, 1 h).

Table 1. Pore morphology of the film.

Sample	BET Surface Area (m^2/gm)	DA Pore Size (Å)	MicroporeVolume(cc/gm)
Alumina (450 °C, 1 h)	220	10.4	0.200
Alumina (450 °C, 6 h)	200.4	10.8	0.177
Alumina (900 °C, 1 h)	186	12.2	0.139

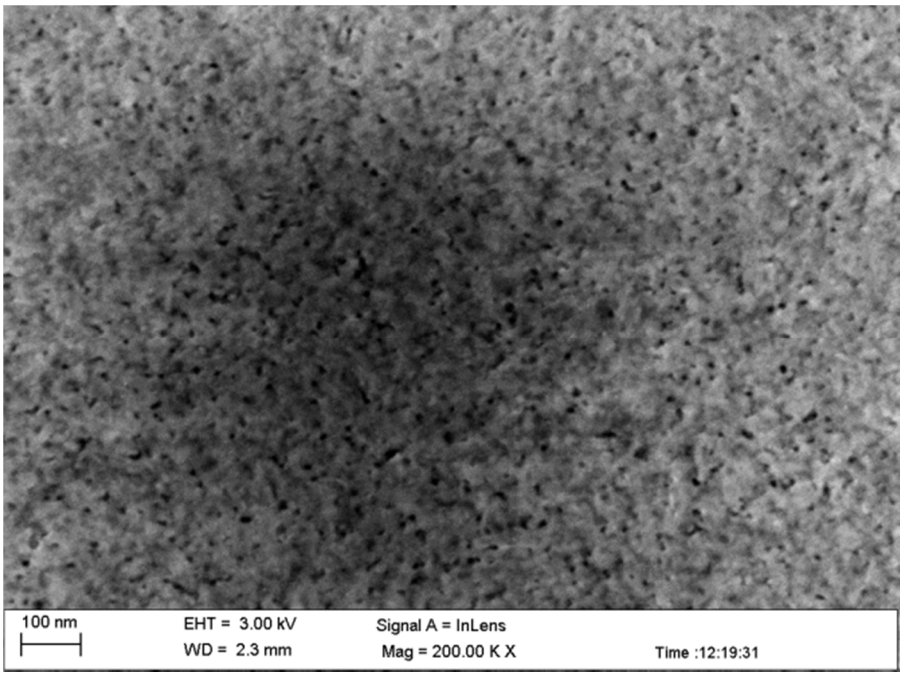

Figure 3. Scanningelectronmicrograph of the top surfaceofthe γ-Al_2O_3 film.

2.3. Fabrication of the Parallel Plate Capacitive Sensors

Capacitive sensors from four different sensing areas—C_{p1}, C_{p2}, C_{p3} and C_{p4}—were fabricated on the alumina substrates. The details of geometrical parameters and sintering temperature of each capacitor are shown in Table 2. The bottom gold electrode on each substrate was deposited by the screen printing method using a manual screen printer. Screen printing uses the stencil method to print the predefined electrode design on the screen. A screen of different electrode pattern was designed using PCB making software and the stencil of the screen printer with polyester fabric was made in the lab.

Table 2. Details of different types of the sensors fabricated.

Sample	C_{p1}	C_{p2}	C_{p3}	C_{p4}
Substrate size (mm)	19 × 19 × 1	19 × 19 × 1	19 × 19 × 1	10 × 10 × 1
Top electrode (mm)	11 × 10	9 × 8	6 × 6	3 × 2
Bottomelectrode	16 × 16	14 × 14	8 × 8	5 × 6
Electrode sintering	900 °C, 1 h	900 °C, 1 h	900 °C, 1 h	900 °C, 1 h
Sensing film	450 °C, 3 h	450 °C, 3 h	450 °C, 3 h	450 °C, 3 h
Sensing area (mm^2)	110	72	36	6
Film thickness (μm)	~6	~6	~6	~6

A thin film of binder mixed alumina sol was deposited on the gold printed alumina substrate by a desktop computer interfaced automatic Single Dip Coatinginstrument (Model: SDC-2007C, Apex Instruments Co. Pvt. Ltd., Kolkata, India). The substrate was dipped in the prepared sol at a dipping speed of 60 mm/m, wet time 30 s and then pulled out at a speed of 30 mm/m. The substrate was kept for 1 m in the solution before being pulled off. Deposited thin film was dried at 80 °C for nearly 5 min. The steps of film deposition over the substrates were repeated six times.

When the film was dried, a second gold electrode was screen printed on the sensing film. The top electrode is made macroporous with average pore size (~1–7 μm), which is much larger than the average pore size of the sensing film. The schematic of film deposition of γ-Al_2O_3 on gold plate by the sol-gel method is shown in Figure 4.

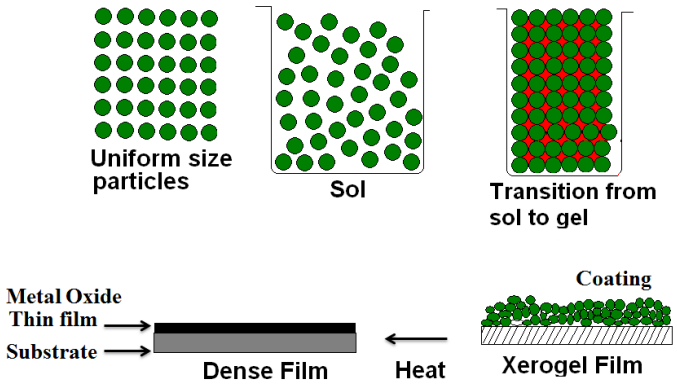

Figure 4. Schematic diagram of the film deposition on the gold electrode.

The red dots in the schematic indicate the formation of pores after sintering. Finally, two terminals are soldered at the top and the bottom electrodes for the electrical connection of the sensor. Precautions were taken to minimize the variation of the film thickness among sensors with the help of a software controlled automatic dipcoater. All the four sensors have almost identical dielectric films, except the electrode size. Figure 5a shows the schematic and Figure 5b shows the photograph of the sensors fabricated in the laboratory environment.

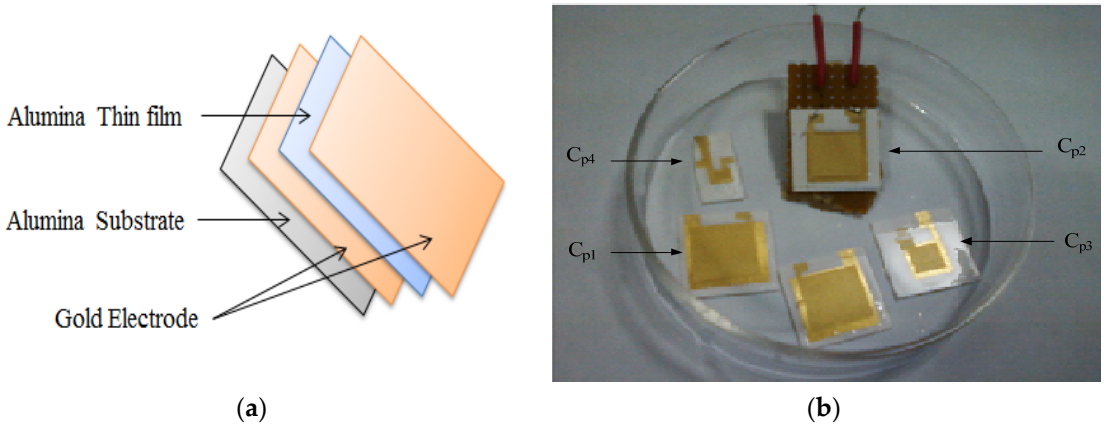

Figure 5. The capacitive sensor with different sensing area (**a**) schematic diagram of the sensor; (**b**) photograph.

3. Determination of the Response Characteristics of the Sensors

The electrical characteristics were determined by holding the sensors inside a rectangular steel chamber, which was made in a local workshop. The inner free space of the chamber is around 100 cc. The chamber has 0.25" inlet and outlet gas pipelines and is connected in series with a reference SHAW dew point meter (model no SADP-TR, Westgate, Bradford, UK) [12]. The reference meter has ahyper thin film parallel electrode metal oxide sensor. The measurement range of the dew point meter is 0–1000 ppm with accuracy ±1 ppm (=0.1%). To refresh the sensor, the chamber was purged with dry N_2 gas at the flow rate of 4–6 L/m. Refreshing continues till the reference meter indicates an initial concentration of around 3 ppm moisture in the moist gas (moisture content of the dry gas cylinder). The desired moist gas concentration was achieved by mixing the commercial dry N_2 gas with water vapor at room temperature (25 °C). The concentration level of the moisture in the moist gas exposed to the sensors varied from 3 to 100 ppm. All the four sensors in the chamber were connected to the Impedance analyzer (4294 A) with a nearly 1 m long shielded wire. The wire was a Teflon insulated multiconductor with capacitance 79 pF/m. For proper shielding, the sensors were held in the grounded metallic chamber. The impedance analyzer was interfaced with a personal computer PC with the help of IEEE 488 interface bus. The input ac excitation for each sensor was of 500 mV (rms) and frequency 1 kHz. The observations of the capacitance values in the Cp-D mode of the impedance analyzer for C_{p1} and C_{p4} with moisture variation from 3 to 100 ppm are shown in Figure 6. The initial capacitance value of each sensor at dry humidity (3 ppm) is different. This difference of the base value is due to the fact that the effective cross-sectional area of each sensor is different. The pore morphology also influences the capacitance value but all the four sensors have identical morphology [1,2]. It is observed in Figure 6 that as the moisture concentration increases, the capacitance value increases but the change in capacitance for C_{P1} and C_{P4} for the same moisture range is significantly different. The highest (46.4%) and the minimum sensitivities (2.9%) are shown by C_{p1} and C_{p4} respectively. When a sensor is exposed to a certain moisture level, the water molecules in cluster form condense on the porous surface and then condense in the voids through capillary condensation in the micropores. As a result, the pores are filled up, causing an increase in the effective dielectric of the sensor. The size of water cluster depends on the moisture concentration. At saturation condition, when the pores are completely filled up, the capacitance value reaches the maximum. Since the sensor is exposed to a very low moisture concentration, the pores are partially filled and hence, the capacitance value continues to increase.

To determine the response (t_r) and the recovery time (t_c), the transient response curve of the sensor C_{p1} for the step change in moisture concentration from 3 to 100 ppm is shown in Figure 7. Such an instantaneous step change of moisture rarely occurs in practice but we have considered a

worstcase scenarioin determining the transient response curve. The sensor takes a very short time, 29 s, to increase the capacitance value from 10 to 90% of its maximum value. During recovery, the sensor was refreshed by dry nitrogen gas to decrease the moisture concentration from 100 ppm to 3 ppm. The capacitance value of the sensor decreases with the decrease in moisture concentration as shown in Figure 7. The recovery time of the sensor is defined as the time taken by the sensor to decrease the capacitance value from maximum to 10% value and it is ~87 s. For the sensor C_{p2}, the response time is 28 s and the recovery time is 85 s. The response and the recovery time depend on the pore morphology, and the thickness of the sensing film. The humidity sensor which works on the adsorption and desorption principle, takes more time to desorb than to adsorb the moisture in the pores. It is observed that the output of the sensor is stable and recovers fully, when the sensor is refreshed by dry N_2 gas. Because of the small sensitivity of C_{p3} and C_{p4}, t_r and t_c of these sensors are not determined.

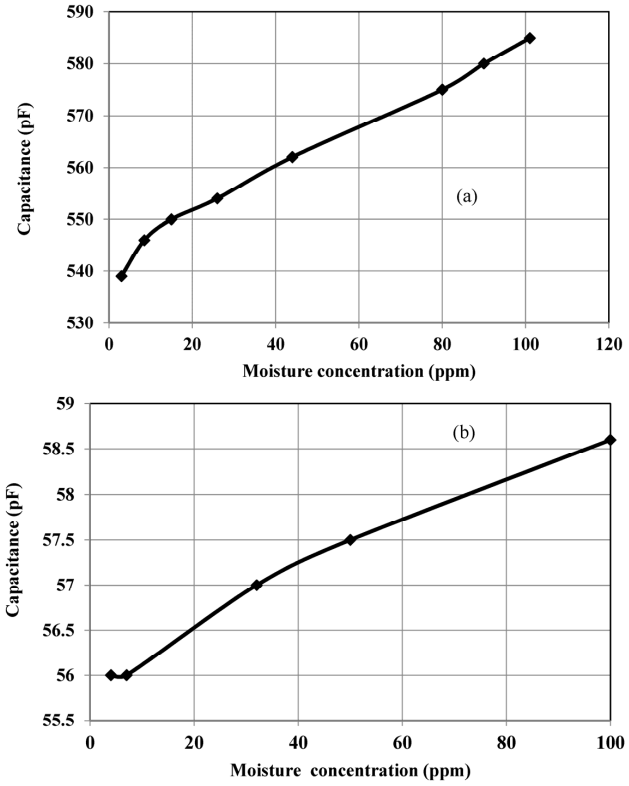

Figure 6. Capacitive response of the sensors (**a**) C_{p1}; (**b**) C_{p4}.

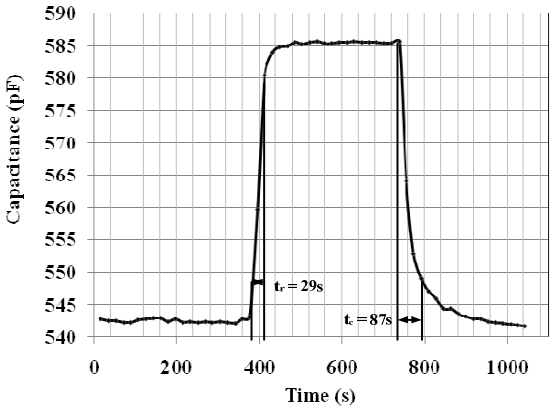

Figure 7. Transient response of the sensor C_{p1}.

4. Results and Discussion

For a parallel plate capacitive sensor, the effective capacitance in the presence of moisture can be represented by [8,22]

$$C_{eff} = \varepsilon_0 \varepsilon_{eff} \frac{A}{d} + C_f \tag{1}$$

where ε_0 is the permittivity of the free space, A is the area of the cross-section of the electrode, d is the thickness of the film, ε_{eff} is the relative dielectric constant of the moist dielectric film, and C_f is the capacitance due to fringing field. The fringing field capacitor will be negligible since the electrode size (A) is much larger than the gap between the electrodes (d) [8]. Therefore, the capacitance of the sensor can be approximately represented by

$$C_{eff} = \varepsilon_0 \varepsilon_{eff} \frac{A}{d} \tag{2}$$

The effective dielectric constant of the capacitor (γ-Al_2O_3) can be approximately given by Looyang's empirical equation as [5,6],

$$\varepsilon_{eff}^{1/3} = \gamma\left(\varepsilon_w^{1/3} - \varepsilon_a^{1/3}\right) + \varepsilon_a^{1/3} \tag{3}$$

where γ is the fractional volume of water adsorbed by the porous film, and ε_w is the dielectric constant of water. The fractional volume of water adsorbed in the porous film depends on the pore morphology. The well-known equation for the Kelvin radius gives us useful information about the desired pore morphology. It is reported that theoretically, the pore size as obtained from the Kelvin equation for sensing moisture in ppm should be below 10 Å [8,26]. The average pore size of the fabricated film as shown in Table 1 is 12.2 Å (γ-Al_2O_3sintered initially at 450 °C and then at 900 °C for 1 h), which is close to the theoretical value.

The sensitivity (S) of a sensor can be defined as [1,2,20,27]

$$S = \frac{C_u - C_l}{C_l} \tag{4}$$

$$S = \frac{C_u - C_l}{RH_u - RH_l} \tag{5}$$

$$S = \frac{\frac{C_u - C_l}{C_l}}{RH_u - RH_l} \tag{6}$$

where C_u and C_l are the upper and the lower limit of the capacitance values of the sensor, RH_u and RH_l are the upper and the lower limit of humidity (%RH or ppm). The sensitivity represented by Equation (5) is more suitable in such a situation when the sensor has approximately linear response [20]. The output of the sensor is approximately linear (R^2 = 0.95, for perfect linear response R^2 = 1). Equation (5) is more usable to understand the performance of the sensor since it provides information about the input and the output parameters, but in Equation (4), the reader does not have an idea about the type of input parameter and its range.

The sensitivity parameters of four sensors have been determined using Equation (5). The sensitivity values of all the four sensors in the range 3–100 ppm are plotted with the variation of the cross-sectional area. It is observed in Figure 8 that the sensitivity increases almost linearly with the increase in effective area. When the effective cross-sectional area increases, more water molecules are adsorbed in the nanostructured porous film, resulting in an increase in effective dielectric constant.

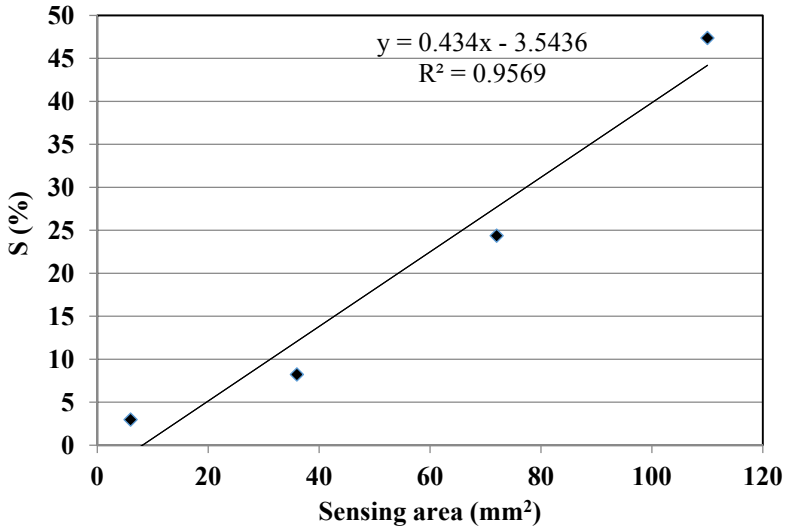

Figure 8. Variation of sensitivity with electrode area for 3–100 ppm moisture.

5. Sensitivity Enhancement by Connecting Two Capacitors in Parallel Fabricated on theSame Substrate

It has been investigated in the previous section that by keeping the pore morphology of the nanostructured film identical, the sensitivity can be increased by simply increasing the electrode area of the capacitor. However, if the electrode area increases, the size of the device will increase and it will create a problem to package the sensor in a small sample chamber. However, if we make two identical parallel plate capacitors on both sides of the alumina substrate, and connect them in parallel, the sensitivity becomes almost double. Additionally, the size of the device remains unchanged and the costly sensing film which is deposited on the opposite side can be effectively utilized. This is because, when thin film is deposited on the gold-plated electrode by the dip coating method, the film deposited on the opposite side of the alumina substrate remains unused [8,12–22]. This issue has not been addressed by previous reported work. Thus, a novel structure which consists of two identical capacitors on each side of the alumina substrate has been fabricated. In addition to this, if the sensitivity enhancement is not an issue for a particular sensor, the opposite capacitor can be used as a reference capacitor, which can be used to minimize the offset capacitance as well as any temperature error of the main sensor, provided the reference capacitor is covered by a hydrophobic film such as Teflon. If C1 is the parallel plate capacitor at one side of the substrate and C2 is another capacitor on the opposite side, then the equivalent capacitance, when both of them are connected in parallel, is C3 = C1 + C2. In comparison to the method of sensitivity enhancement by the preparation of nanostructure, this method is simple, less time consuming, less costly and mass producible.

Procedures to Fabricate the Device

The steps of the fabrication process remain the same as in the case of a single sided capacitive trace moisture sensor [6–8,12–22]. Two gold electrodes are deposited on each side of an alumina substrate (19 mm × 19 mm × 1 mm) by the screen printing method. The size of each electrode is 16 mm × 16 mm. The electrodes are sintered at 900 °C for 1 h in a furnace. Thin film of γ-Al_2O_3 is deposited on each electrode by the dip coating method under a similar deposition condition as discussed in Section 2.3. Film is deposited on both sides simultaneously. Finally, the top gold electrode is deposited on each side of the film. The dimension of the top electrode is 12 mm × 14 mm. However, due to manual fabrication, there may be minor variation of the electrode size of C1 and C2 respectively. Both the capacitances are connected in parallel. The response characteristics of C1, C2 and C3 are determined with the variation of moisture in the range of 3–108 ppm.The capacitive response curve

of the sensor C2 with the variation of moisture is shown in Figure 9a. The capacitive response of C3 when both C1 and C2 are connected in parallel is shown in Figure 9b.

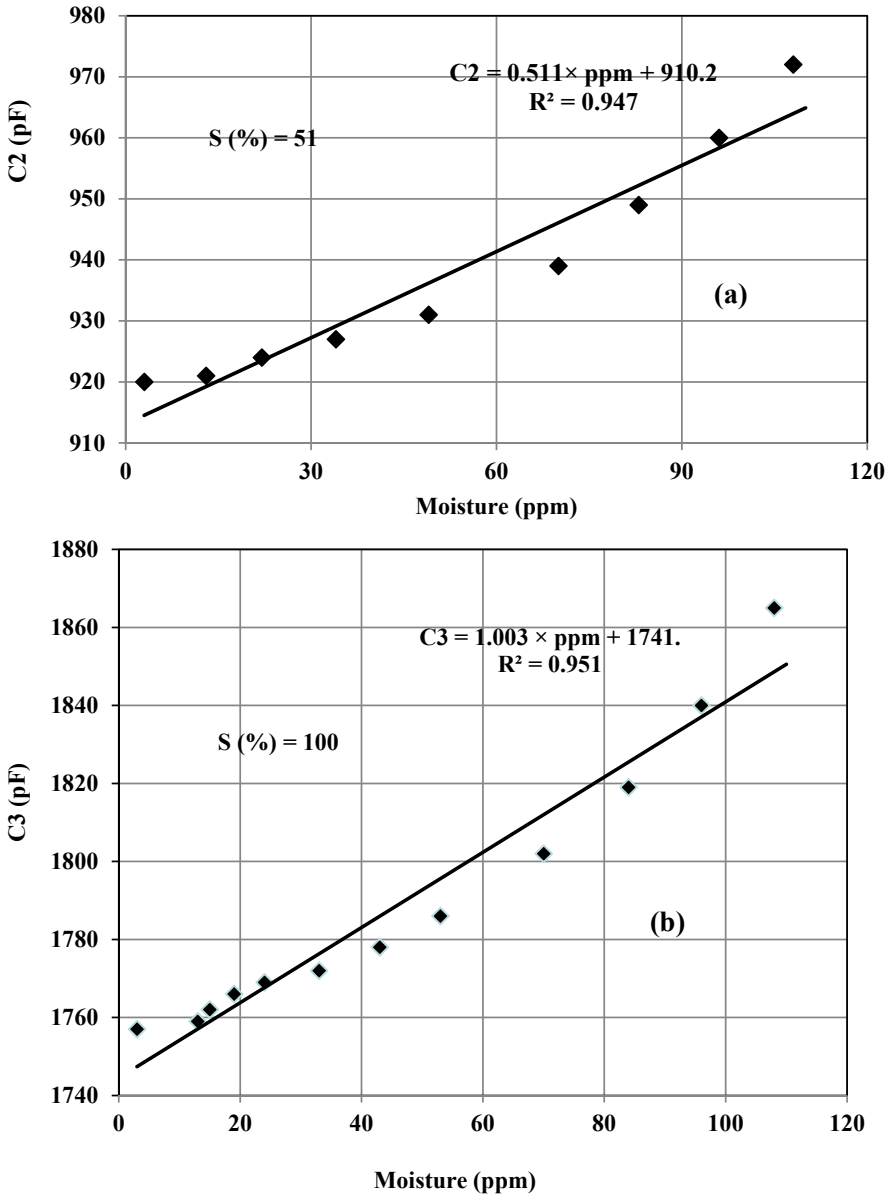

Figure 9. The response curve of the proposed sensor structure connected in parallel, (**a**) C2; the capacitor on the bottom side (**b**) C3 = C1 + C2.

It is observed that in the case of C3, the overall capacitance change for the same moisture range becomes almost double. This sensitivity enhancement is obtained by simply connecting the two capacitors in parallel without modifying the surface area or the thickness of the film. The correlation coefficient of the actual response curve from the linear fitted curve is 0.95, which is close to the desired value of 1. Linearity is always a desirable characteristic of a sensor for ease of calibration. For a linear response, only two calibration points are required to calibrate the reading. The conversion from a scale reading to the corresponding measured value of input moisture is most convenient if it is required to multiply a fixed constant rather than to refer to a nonlinear calibration curve or to compute from a nonlinear calibration equation.Hysteresis is another important parameter of a sensor. When a sensor is employed for moisture measurement in any application, the moisture level in the environment may increase or decrease. Ideally, the sensor should give the same capacitance at the

same moisture level when approached in both directions. For a sensor withhysteresis error, different reading results for a particular moisture level are given, depending on whether the moisture level is applied from lower or higher values. The hysteresis plot for both increase and decrease in moisture from 13 to 108 ppm for C3 is shown in Figure 10. The maximum deviation of the capacitance value for the forward and reverse cycle of moisture is around 0.45%. The response and recovery times of C3 determined from the transient response curve for a 3–108 ppm step change in moisture are 28 s and 40 s respectively. The repeatability of the capacitive response of C3 for three similar step changes in moisture concentration is shown in Figure 11. The repeatability error is caused by the inability of the sensor to give the same capacitance under similar step change in moisture. The maximum repeatability error of the sensor output is ~0.2% and the standard deviation of the successive peaks is 0.7. Experiments were also performed to study the signal frequency effect on the capacitance values, by varying the frequency from 100 Hz to 100 kHz at fixed 80 ppm moisture. The rate of change of the capacitance value at lower frequency—below 20 kHz—is much higher than the frequency above 20 kHz. Therefore, the ac signal with frequency above 20 kHz is suitable to avoid the frequency dependency capacitance change. This is due to the fact that, when the sensor is interfaced with an electronic circuit for displaying the moisture value, the minor change in excitation frequency does not affect the reading of the meter. High capacitance change at lower frequency is due to the combined effect of dielectric adsorption capacitance and the double layer capacitance. At higher frequency, the effect of double layer capacitance is insignificant [33].

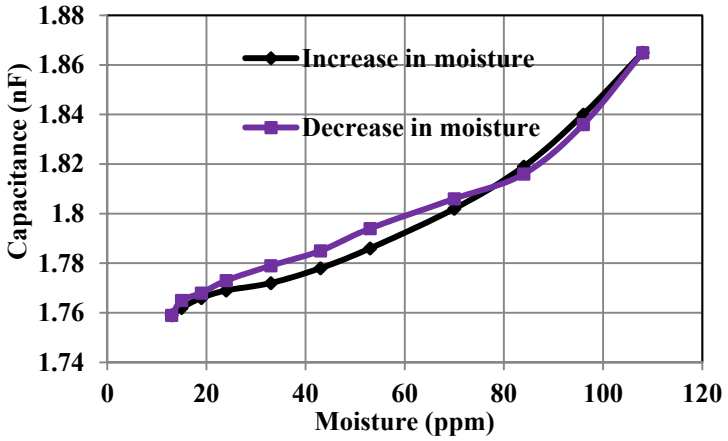

Figure 10. Hysteresis plot of the sensor C3.

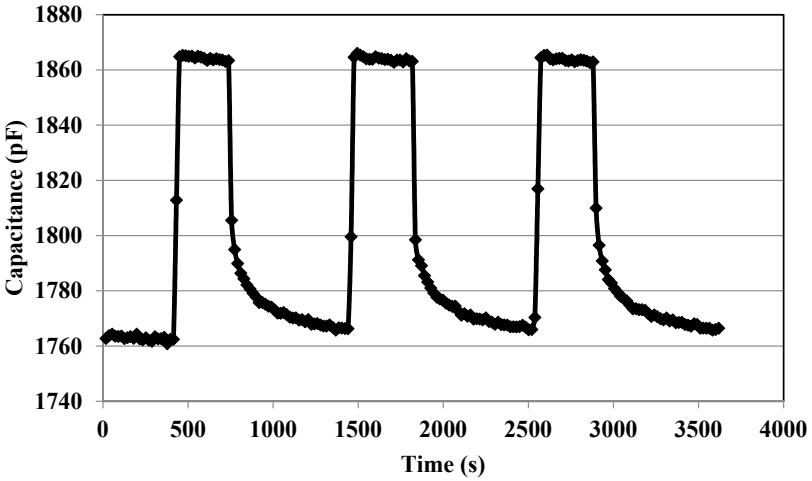

Figure 11. Repeatability of the sensor C3.

Investigation is needed to study the drift due to aging [2]. Our experience shows that if the sensor is kept in drying agent (molecular sieve) as practiced in a commercial dew point meter (SHAW), the reading will be stable for a long time [10,11]. However, if there is a drift in the output, it can be reduced by heating the sensor at a temperature of around 400 °C. Drift is caused due to deposition of residual impurity from the N_2 gas or due to gradual change in γ phase to γ-$Al_2O_3.H_2O$ (boehmite). This causes volume expansion of the oxide, resulting in a gradual decrease in surface area and porosity [2]. The sensor does not show any drift due to the change in working temperature [9,18,19,23]. Comparison of the characteristics of the single sided and double sided sensor with the reading of the commercial dew point meter is shown in Table 3.

Table 3. Comparison of the response characteristics of different sensors.

Sensor	Measurement Range (ppm)	S (%)	t_r (s)	t_c (s)
C_{p1}	3–100	46.4	29	87
C_{p2}	3–100	16.4	28	85
C3	3–100	100	28	40
SHAWdew point [19]	0–1000	100.5	258	-

6. Conclusions

The present work deals with the fabrication of capacitive porous alumina-based sensors with different sensing areas for sensing humidity in ppm. The pore morphology of the sensing layer of each sensor is identical. The characteristics of the moisture sensors were examined for 3 to 100 ppm moisture content in dry gas. We have found that a moisture sensor with a larger effective area has higher sensitivity in a lower range. Pore morphology, thickness of the film and the sensing area play an important role for the sensitive detection of humidity at trace level. The parallel plate sensor provides a better solution for trace moisture detection. In comparison to the conventional interdigitated sensor, the parallel plate sensor with very small size may sense humidity at the %RH level. We have also discussed another unique structure consisting of capacitors on each side of the substrate to enhance the sensitivity for trace level moisture detection. This double sided capacitor structure is easy to fabricate and it can enhance sensitivity greatly without affecting the overall size. It may be possible to obtain a measurementbelow 3 ppm, but due to the lack of a testing facility, an experiment was not conducted. Further work could test the sensor's ability to measure moisture in GIS or transformer oil.

Acknowledgments: Authors would like to thank the funding agency DRDO for providing the financial support.

Author Contributions: L.K. performed the experimental work under the supervision of T.I. S.C.M. gave the valuable suggestion to conduct experiments.

Conflicts of Interest: The authors declare no conflict of interest.

References

1. Fenner, R.; Zdankiewicz, E. Micromachined water vapor sensors: A review of sensing technologies. *IEEE Sens.* **2001**, *1*, 309–317. [CrossRef]
2. Feng, S.; Chen, X.; Chen, J.; Hu, J. A novel humidity sensor based on alumina nanowire films. *J. Phys. D Appl. Phys.* **2012**, *45*, 225305. [CrossRef]
3. Tetelin, A.; Pouget, V.; Lachaud, J.-L.; Pellet, C. Dynamic behavior of a chemical sensor for humidity level measurement in human breath. *IEEE Trans. Inst. Meas.* **2004**, *53*, 1262–1267. [CrossRef]
4. Fagan, J.G.; Amarakoon, V.R.W. Reliability and reproducibility of ceramic sensors, part III, humidity sensors. *Am. Ceram. Soc. Bull.* **1993**, *72*, 119–130.
5. McMillan, G.K.; Douglas, M. *Process/Industrial Instruments and Controls Handbook*, 5th ed.; Tata McGraw Hill Education Private Limited: Patel Nagar, New Delhi, India, 2009; pp. 4237–4247.
6. Blanka, T.A.; Eksperiandova, L.P.; Belikov, K.N. Recent trends of ceramic humidity sensors development: A review. *Sens. Actuators B* **2016**, *228*, 416–442. [CrossRef]

7. Islam, T.; Nimal, A.T.; Mittal, U.; Sharma, M.U. A micro interdigitated thin film metal oxide capacitive sensor for measuring moisture in the range of 175–625 ppm. *Sens. Actuators B* **2015**, *221*, 357–364. [CrossRef]
8. Mahboob, M.R.; Zargar, Z.H.; Islam, T. A sensitive and highly linear capacitive thin film sensor for trace 173 moisture measurement in gases. *Sens. Actuators B* **2016**, *228*, 658–664. [CrossRef]
9. Funke, H.H.; Grissom, B.L.; McGrew, C.E.; Raynor, M.W. Techniques for the measurement of trace moisture in high-purity electronic specialty gases. *Rev. Sci. Instrum.* **2003**, *74*, 3909–3933. [CrossRef]
10. Neumeier, S.; Echterhof, T.; Olling, R.; Pfeifer, H.; Simona, U. Zeolite based trace humidity sensor for high temperature applications in hydrogen atmosphere. *Sens. Actuators B* **2008**, *134*, 171–174. [CrossRef]
11. Islam, T.; Kumar, L.; Khan, S.A. A novel sol-gel thin film porous alumina based capacitive sensor for measuring trace moisture in the range of 2.5 to 25 ppm. *Sens. Actuators B* **2012**, *173*, 377–384. [CrossRef]
12. De Lange, M.F.; Vlugt, T.J.H.; Gascon, J.; Kapteijn, F. Adsorptive characterization of porous solids: Error analysis guides the way. *MicroporousMesoporous Mater.* **2014**, *200*, 199–215. [CrossRef]
13. Brinker, C.J.; Scherer, G.W. *Sol–Gel Science*; Academic Press: San Diego, CA, USA, 1990.
14. SHAW Moisture Meters (UK) Ltd. Westgate Bradford. BD13SQ. Available online: www.shawmeters.com (accessed on 15 March 2017).
15. General Electric. Moisture and Humidity Measurement. Available online: www.ge-mcs.com (accessed on 15 March 2017).
16. Hashiguchi, K.; Lisak, D.; Cygan, A.; Ciuryło, R.; Abea, H. Wavelength-meter controlled cavity ring-downspectroscopy: High-sensitivity detection of trace moisture in N_2 at sub-ppb levels. *Sens. Actuators A* **2016**, *241*, 152–160. [CrossRef]
17. Kapaa, P.; Pana, L.; Bandhanadhama, A.; Fanga, J.; Varahramyana, K.; Davis, W.; Ji, H.F. Moisture measurement using porous aluminum oxide coated microcantilevers. *Sens. Actuators B* **2008**, *134*, 390–395. [CrossRef]
18. Pandey, M.; Mishra, P.; Saha, D.; Sengupta, K.; Jain, K.; Islam, S.S. Nanoporous alumina (c- and a-phase) gel cast thick film for the development of trace moisture sensor. *J. Sol-Gel Sci. Technol.* **2013**, *68*, 317–323. [CrossRef]
19. Ohira, S.; Goto, K.; Toda, K.; Dasgupta, P.K. A capacitance sensor for water: Trace moisture measurement ingases and organic solvents. *Anal. Chem.* **2012**, *84*, 8891–8897. [CrossRef] [PubMed]
20. Doeblin, E.O. *Measurement Systems: Application and Design*, 4th ed.; Tata McGraw Hill: New Delhi, India, 2002; p. 198.
21. Basu, S.; Saha, M.; Chatterjee, S.; Mistry, K.; Bandyopadhay, S.; Sengupta, K. Porous ceramic sensor for measurement of gas moisture in the ppm range. *Mater. Lett.* **2001**, *49*, 29–33. [CrossRef]
22. Saha, D.; Sengupta, K. Trace moisture detection in oil filled transformer by ceramic sensor. *Mater. Sci. Eng.* **2015**, *73*, 012022. [CrossRef]
23. Chen, Z.; Jin, M.C. An Alpha-Alumina Moisture Sensor for Relative and Absolute Humidity Measurement. In Proceedings of the 1992 IEEE Industry Applications Society Annual Meeting, Houston, TX, USA, 4–9 October1992; Volume 2, pp. 1668–1675.
24. Islam, T.; Mahboob, R.; Khan, S.A. A simple MOX vapor sensor on polyimide substrate for measuring humidity in ppm Level. *IEEE Sens.* **2015**, *15*, 3004–3013. [CrossRef]
25. Kima, Y.; Junga, B.; Leea, H.; Kimb, H.; Leeb, K.; Park, H. Capacitive humidity sensor design based on anodic aluminum oxide. *Sens. Actuators B* **2009**, *141*, 441–446. [CrossRef]
26. Islam, T.; Khan, U.A.; Akhtar, J.A.; Rahman, M.Z.U. A digital hygrometer for trace moisture measurement. *IEEE Trans. Ind. Electr.* **2014**, *61*, 5599–5605. [CrossRef]
27. Bakhoum, E.G.; Cheng, M.H.M. High-accuracy miniature dew point sensor and instrument. *IEEE Sens. J.* **2015**, *15*, 1482–1488. [CrossRef]
28. Batumalay, M.; Harun, S.W.; Irawati, N.; Ahmad, H.; Arof, H. A study of relative humidity fiber-optic sensors. *IEEE Sens. J.* **2015**, *15*, 1945–1950. [CrossRef]
29. Babaei, F.H.; Rahbarpour, S. Alteration of pore size distribution by sol–gel impregnation for dynamic range and sensitivity adjustment in Kelvin condensation-based humidity sensors. *Sens. Actuators B* **2014**, *191*, 572–578. [CrossRef]
30. Lopez, F.M.; Briand, D.; Rooij, N.F. Decreasing the size of printed comb electrodes by the introduction of a dielectricinterlayer for capacitive gas sensors on polymeric foil: Modeling and fabrication. *Sens. Actuators B* **2013**, *189*, 89–96. [CrossRef]

31. Whelan, A.M. Sol-Gel Sensors. In *Sol-Gel Materials for Energy, Environment and Electronic Applications*; Springer: Berlin, Germany; pp. 121–153.
32. Yoldas, B.E. Design of sol-gel coating media for ink-jet printing. *J. Sol-Gel Sci. Technol.* **1998**, *13*, 147–152. [CrossRef]
33. Islam, T.; Rahman, Z.U. Investigation of the electrical characteristics on measurement frequency of a thin-film ceramic humidity sensor. *IEEE Trans. Instrum. Meas.* **2016**, *65*, 694–702. [CrossRef]

© 2017 by the authors. Licensee MDPI, Basel, Switzerland. This article is an open access article distributed under the terms and conditions of the Creative Commons Attribution (CC BY) license (http://creativecommons.org/licenses/by/4.0/).